

Aging-associated metabolic disorder induces Nox2 activation and oxidative damage of endothelial function

Article

Published Version

Creative Commons: Attribution-Noncommercial-No Derivative Works 4.0

Open access

Fan, L. M., Cahill-Smith, S., Geng, L., Du, J., Brooks, G. and Li, J.-m. ORCID: <https://orcid.org/0000-0002-3294-3818>
(2017) Aging-associated metabolic disorder induces Nox2 activation and oxidative damage of endothelial function. Free Radical Biology and Medicine, 108. pp. 940-951. ISSN 0891-5849 doi: 10.1016/j.freeradbiomed.2017.05.008 Available at <https://centaur.reading.ac.uk/70338/>

It is advisable to refer to the publisher's version if you intend to cite from the work. See [Guidance on citing](#).

Published version at: <https://doi.org/10.1016/j.freeradbiomed.2017.05.008>

To link to this article DOI: <http://dx.doi.org/10.1016/j.freeradbiomed.2017.05.008>

Publisher: Elsevier

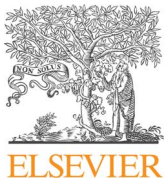
All outputs in CentAUR are protected by Intellectual Property Rights law, including copyright law. Copyright and IPR is retained by the creators or other copyright holders. Terms and conditions for use of this material are defined in the [End User Agreement](#).

www.reading.ac.uk/centaur

CentAUR

Central Archive at the University of Reading

Reading's research outputs online



Original article

Aging-associated metabolic disorder induces Nox2 activation and oxidative damage of endothelial function

Lampson M. Fan^{a,1}, Sarah Cahill-Smith^{b,1}, Li Geng^c, Junjie Du^b, Gavin Brooks^c, Jian-Mei Li^{c,*}^a Division of Cardiovascular Medicine, University of Oxford, UK^b Faculty of Health and Medical Sciences, University of Surrey, UK^c Institute for Cardiovascular and Metabolic Research, School of Biological Sciences, University of Reading, UK

ARTICLE INFO

Keywords:
 NADPH oxidase
 Knockout mice
 Oxidative stress
 Aging
 Metabolic disorder
 Endothelial dysfunction

ABSTRACT

Oxidative stress attributable to the activation of a Nox2-containing NADPH oxidase is involved in the development of vascular diseases and in aging. However, the mechanism of Nox2 activation in normal aging remains unclear. In this study, we used age-matched wild-type (WT) and Nox2 knockout (KO) mice at 3–4 months (young); 11–12 months (middle-aged) and 21–22 months (aging) to investigate age-related metabolic disorders, Nox2 activation and endothelial dysfunction. Compared to young mice, middle-aged and aging WT mice had significant hyperglycaemia, hyperinsulinaemia, increased systemic oxidative stress and higher blood pressure. Endothelium-dependent vessel relaxation to acetylcholine was significantly impaired in WT aging aortas, and this was accompanied by increased Nox2 and ICAM-1 expressions, MAPK activation and decreased insulin receptor expression and signaling. However, these aging-associated disorders were significantly reduced or absent in Nox2KO aging mice. The effect of metabolic disorder on Nox2 activation and endothelial dysfunction was further confirmed using high-fat diet-induced obesity and insulin resistance in middle-aged WT mice treated with apocynin (a Nox2 inhibitor). In vitro experiments showed that in response to high glucose plus high insulin challenge, WT coronary microvascular endothelial cells increased significantly the levels of Nox2 expression, activation of stress signaling pathways and the cells were senescent, e.g. increased p53 and β -galactosidase activity. However, these changes were absent in Nox2KO cells. In conclusion, Nox2 activation in response to aging-associated hyperglycaemia and hyperinsulinaemia plays a key role in the oxidative damage of vascular function. Inhibition or knockout of Nox2 preserves endothelial function and improves global metabolism in old age.

1. Introduction

Age is recognized as a major risk factor for cardiovascular diseases. High prevalence of obesity and insulin resistance in an aging population has led to a rapid increase in type-2 diabetes and cardiovascular diseases [1–3]. An early feature in the development of metabolic and cardiovascular diseases is the progressive endothelial dysfunction attributable to increased reactive oxygen species (ROS) production by a Nox2-containing NADPH oxidase [2,4–8]. Oxidative stress causes DNA damage, alters transcriptional machinery and promotes inflammatory gene expressions. All these are key factors that further accelerate vascular aging [2].

NADPH oxidase is a multicomponent enzyme. The catalytic subunit

of NADPH oxidase has been found to have 7 isoforms (Nox1–5, and Duox 1–2) [9,10]. Among these Nox isoforms, Nox2 is highly expressed in both inflammatory phagocytic cells and vascular endothelial cells [9,10]. Unlike the other Nox isoforms, Nox2 requires p22^{phox} and several regulatory subunits i.e. p40^{phox}, p47^{phox}, p67^{phox} and rac1 for O_2^- production [11]. In response to stimuli, such as high glucose, oxidized LDL and inflammatory cytokines, endothelial Nox2 is activated and produces excessive levels of ROS, which outstrips the endogenous antioxidant defense and causes oxidative damage to the endothelium and the organs [7,8]. Transgenic mice with endothelial-specific Nox2 overexpression had high levels of ROS production and ERK1/2 activation in the endothelium [7], and there is a close relationship between the levels of endothelial oxidative stress and the

Abbreviations: CMEC, coronary microvascular endothelial cells; DHE, dihydroethidium; HFD, high fat diet; IR, insulin receptor; KO, knockout; ROS, reactive oxygen species; SABG, senescence-associated β -galactosidase; SOD, superoxide dismutase; WT, Wild-type

* Corresponding author.

E-mail address: jian-mei.li@reading.ac.uk (J.-M. Li).

¹ Equal contribution of these two authors.

degree of insulin resistance and cardiovascular disorders found in experimental animals and in humans [4,6,12]. However, the mechanism of Nox2 activation in normal aging remains unclear.

In this study, we used littermates of age-matched wild-type (WT) and Nox2 knockout (Nox2KO) mice in young (3–4 m); middle-aged (11–12 m) and old age (21–22 m) to investigate the mechanism of aging-associated Nox2 activation and global oxidative stress. In particular, we examined the relationship between the levels of aging-related glucose metabolic disorders and endothelial Nox2 activation in aorta inflammation, decline of insulin receptor expression and endothelial dysfunction. The critical role of metabolic disorder in Nox2 activation and endothelial dysfunction was further examined using a model of high-fat diet-induced obesity and insulin resistance in middle-aged WT mice treated with or without apocynin (a Nox2 inhibitor). We also examined the mechanisms of high glucose and insulin-induced Nox2 activation and redox-signaling in endothelial cell senescence and apoptosis using coronary microvascular endothelial cells (CMEC) isolated from WT and Nox2KO mice. Our study for the first time demonstrated a crucial role of global Nox2 activation in response to aging associated glucose metabolic disorders (i.e. hyperglycaemia and hyperinsulinaemia) causing inflammation and oxidative damage of endothelial function and insulin receptor function in major vessels. Inhibition or knockout of Nox2 helps to preserve endothelial function and improves global metabolism in old age.

2. Materials and methods

2.1. Reagents

Polyclonal antibodies against Nox1, Nox2, Nox4, p22^{phox}, p40^{phox}, p47^{phox}, p67^{phox}, rac1, insulin receptors (IR α and IR β) were from Santa Cruz Biotechnology. Antibodies to phospho-ERK1/2, phospho-p38MAPK, phospho-JNK and phospho-Akt^{ser473} were from Cell Signaling Technology. DHE (dihydroethidium) and 5-(and 6)-chloromethyl-2',7'-dichlorodihydrofluorescein diacetate (DCF) were from Invitrogen (UK). All other reagents and chemicals were from Sigma unless stated otherwise.

2.2. Animals

All studies were performed in accordance with the protocols approved by the Home Office under the Animals (Scientific Procedures) Act 1986, UK. Nox2 knockout mice on a C57BL/6J background were originally obtained from Jackson Laboratory, USA. These mice were generated by insertion of an expression cassette for neomycin resistance into exon 3 of the Nox2 gene (Cybb) and attaching a flanking herpes thymidine kinase gene [13]. Nox2KO mice lack phagocyte superoxide production and manifest an increased susceptibility to infection. Littermates of WT and Nox2KO mice were bred in our institution from heterozygotes and genotyped. Animals were housed under standard conditions with a 12:12 light dark cycle and food and water were available ad libitum. Male mice were randomly grouped and used at young (3–4 m), middle age (11–12 m) and old age (21–22 m). A total of 12–15 mice were used per group. Body weights were measured monthly. The measurement of food intake was for a period of 3 days while the animals were individually housed and repeated every month.

2.3. High-fat diet-induced obesity and insulin resistance in middle-aged mice treated with or without apocynin

Littermates of WT and Nox2KO male mice at 8 m of age were randomly assigned (n=10/per group) to a high-fat diet (HFD group): 45% kcal fat, 20% kcal protein, and 35% kcal carbohydrate (Special Diets Services, UK), or a normal chow diet (control group): 3% kcal fat, 25.9% kcal protein, and 64.8% kcal carbohydrate (LabDiet Ltd., UK) for

16 weeks. Apocynin was supplied in drinking water (5 mM). Food intake and body weights were measured as described above. Mice were used at the age of 12 m.

2.4. Metabolic measurements and intraperitoneal glucose tolerance test (IPGTT)

These were performed as described previously [8]. Serum glucose was measured at 9 a.m. after 8 h of fasting using a blood glucose meter (Accu-Chek, UK). Fasting plasma insulin was measured using a mouse insulin enzyme-linked immunosorbent assay kit (Mercodia Developing Diagnostic, Sweden). Fasting serum cholesterol, FFA, triglyceride, and high-density-lipoprotein (HDL) cholesterol were measured by enzymatic colorimetric assays using an iLab 650 Chemistry System. LDL cholesterol was calculated as the difference between total and HDL cholesterol concentrations based on the Friedewald equation [14]. For the IPGTT, mice were fasted for 8 h before an intraperitoneal injection (IP) of glucose (2 g kg⁻¹ body weight) was administrated. Blood glucose was then measured at 15, 30, 60 and 120 min after injection.

2.5. Blood pressure (BP) and endothelial function assessments

These were performed exactly as described previously [8]. BP was measured by a computer controlled non-invasive tail-cuff BP system (Kent Scientific Corporation, USA) on conscious mice at 10 am, and measurements were recorded by the CODA™ program. The mean of at least 6 successful recordings was used for each mouse. For the assessment of endothelial function, freshly excised thoracic aortic rings (3–4 mm in length) were suspended in an organ bath (ML0146/C-V, AD Instrument Ltd) at 37 °C containing 10 ml of Krebs-Henseleit solution (in mmol/L: NaCl 119, KCl 4.7, KH₂PO₄ 1.2, MgSO₄ 1.2, CaCl₂ 2.5, NaHCO₃ 25, glucose 11.1, pH 7.4) gassed with 95% O₂/5% CO₂. The cumulative dose response to phenylephrine (PE) (1 nmol/L to 10 μmol/L) was assessed first. After washing and re-equilibration, relaxation responses to sodium nitroprusside (SNP, 0.1 nmol/L to 1 μmol/L) or acetylcholine (Ach, 1 nmol/L to 10 μmol/L) were assessed in rings pre-constricted to ~70% of their maximal PE-induced tension. Relaxation was expressed as the percentage of pre-constricted tension. Some experiments were performed in the presence of tiron (10 mmol/L) or the nitric oxide synthase (NOS) inhibitor, N^ω-Nitro-L-arginine methyl ester (L-NAME, 100 μmol/L).

2.6. Coronary microvascular endothelial cell (CMEC) isolation

CMECs were isolated from the hearts of middle-aged (11–12 m) WT and Nox2KO mice according to the method reported previously [15]. Six hearts were used for each CMEC isolation. CMECs were cultured in DMEM supplemented with 10% FBS, EC growth supplement (30 μg/ml), epidermal growth factor (10 ng/ml), vascular endothelial growth factor (0.5 ng/ml), ascorbic acid (1 μg/ml), hydrocortisone (1 μg/ml), L-glutamine (2 mmol/L), penicillin (50 U/ml) and streptomycin (50 μg/ml). CMECs were used at passage 2.

2.7. In situ detection of senescence-associated β-galactosidase (SA β G) activity

The SA β G activity (a cell senescence marker) in cultured CMECs was performed as described previously [16]. Briefly, cells were cultured on chamber slides and treated according to the experimental design. After fixation with 1% ice-cold paraformaldehyde and washing in PBS, cells were incubated with freshly prepared staining buffer containing 40 mmol/L citric acid/sodium (pH 6.0), 0.15 mol/L NaCl, 2 mmol/L MgCl₂, 5 mmol/L potassium ferrocyanide, 1 mg/ml X-gal (5-bromo-4-chloro-3-indolyl β-D-galactoside). The SA β G positive cells (blue) were examined microscopically at $\times 200$ magnification and counted.

2.8. TUNEL assay

The TUNEL assay was performed as described previously [17]. Briefly, endothelial cells were cultured onto the chamber slide, and stimulated with high glucose plus insulin for 24 h. The cells were then washed and fixed in 2% methanol-free formaldehyde/PBS solution, and treated with 0.2% Triton® X-100/PBS solution for 5 min. The TUNEL assay was performed using the DeadEnd fluorometric technique (Promega, UK) following the protocol of the manufacturer and visualised under fluorescence microscopy.

2.9. ROS measurement

The O_2^- production by tissue (or cell) homogenates was measured by three complementary techniques: lucigenin (5 μ mol/L)-chemiluminescence in tissue homogenates (Lumistar, BMG); DHE (2 μ mol/L) fluorescence on tissue sections or DCF fluorescence for cells as described previously [18] and superoxide dismutase (SOD, 200 U/ml)-inhibitable cytochrome c reduction assay [19]. The specificity of detection of O_2^- was confirmed by adding tiron (10 mmol/L), a non-enzymatic O_2^- scavenger. The enzymatic sources of O_2^- production were identified using inhibitors targeting NOS (L-NAME 100 μ mol/L), the mitochondrial complex-1 enzymes (rotenone, 50 μ mol/L), xanthine oxidase (oxypurinol, 250 μ mol/L), flavo-proteins (diphenyleneiodonium, DPI, 20 μ mol/L), or SOD (200 U/ml) before O_2^- measurement. DHE (or DCF) images were captured digitally and acquired using an Olympus BX61 fluorescence microscope. The fluorescence intensity was quantified from at least 5 random fields ($269.7 \times 269.2 \mu$ m) per section with 3 sections/sample and 6 animals/group. Nitric oxide (NO) production was assessed by measuring the concentration of serum nitrite, which is one of the primary stable and nonvolatile breakdown products of NO using the Griess assay kit from Promega UK.

2.10. Immunoblotting

This was performed exactly as described previously [8,20]. The images were captured digitally using a BioSpectrum AC imaging system (UVP, UK), and the optical densities of the protein bands were normalized to the loading control bands and quantified.

2.11. Immunofluorescence microscopy

The experiments were performed exactly as described previously [8,20]. Primary antibodies were used at 1:250 dilution and biotin-conjugated anti-rabbit or anti-goat (1:1000 dilution) were used as secondary antibodies. Specific binding of antibodies was detected by extravidin-FITC or streptavidin-Cy3. Normal rabbit or goat IgG (5 μ g/ml) was used instead of primary antibody as a negative control. Images were acquired with an Olympus BX61 fluorescence microscope system. Fluorescence intensities were quantified as described above.

2.12. Statistical analysis

Statistical analysis was performed using one-way or two-way analysis of variance (ANOVA) followed by Bonferroni post-hoc tests except where it was specified in the figure legend. The data were from at least 9–13 mice/group and expressed as mean \pm SD except where specified in the figure legend. $P < 0.05$ was considered statistically significant.

3. Results

3.1. Aging-associated metabolic disorders and insulin resistance

There was no significant difference in the amount of food intake, heart weight/body weight ratios and serum nitrite levels (an indicator

of NO metabolism) between age groups of WT and Nox2KO mice (Fig. 1A). At young age (3–4 m), there was no significant difference between WT and Nox2KO mice for all of the parameters examined (Fig. 1A–B). However, WT mice had significantly greater body weight, epididymal fat weight and blood pressure starting at middle age (11–12 m) and progressing to old age (21–22 m). Compared to age-matched WT mice, age-related increases in body and epididymal fat weights were significantly reduced in Nox2KO mice. Blood pressure was well maintained in Nox2KO mice without any significant differences between age groups (Fig. 1A).

The levels of fasting serum non-essential free fatty acids (NEFA) and triglyceride were well maintained without significant age-related differences between WT and Nox2KO mice (Fig. 1B). However, the levels of fasting serum total cholesterol, LDL, glucose and insulin increased as age progressed and were statistically significant at old-age in comparison to young mice in WT mice, but not in Nox2KO mice. Insulin resistance in aging WT mice was further confirmed by glucose tolerance tests (Fig. 1C).

3.2. Knockout Nox2 abolished aging-associated increase in ROS production in multiple organs

Age-related systemic oxidative stress was examined by measuring the levels of NADPH-dependent O_2^- production using organ homogenates by lucigenin (5 μ M)-chemiluminescence (Fig. 2). In WT mice, the levels of O_2^- production in different organs varied with the highest levels found in the bone marrow and the liver. There were significant increases in the levels of O_2^- production starting at middle age and progressing to old-age in the heart, lung, liver, kidney, aorta, spleen, fat, brain and the bone marrow (except skeletal muscles) of WT mice, but not in the organs of Nox2KO mice. In fact, the Nox2KO bone marrow, spleen and fat tissue had very little (just detectable) O_2^- production. The skeletal muscle produced low levels of O_2^- production without significant difference between age groups of both WT and Nox2KO mice.

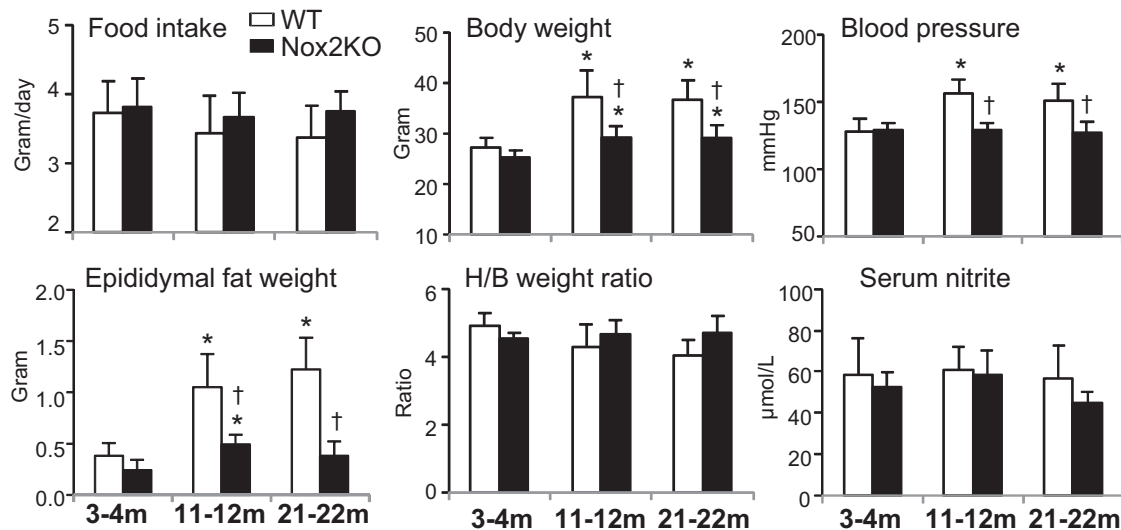
3.3. Aging-associated endothelial dysfunction in WT but not in Nox2KO mice

The vascular function was examined *ex vivo* using freshly isolated aortic sections in an organ bath. There were no significant differences in the vessel contractile responses to phenylephrine (PE) between WT and Nox2KO mice of all age groups (Figs. 3A and 3E). At young age, there were no significant differences in endothelium-dependent vessel relaxation to acetylcholine (Ach) between WT and Nox2KO mice. However, the endothelium-dependent vessel relaxation response to acetylcholine started to reduce at middle-age and was significantly impaired at old age (Fig. 3B), which could be corrected back to levels of the young mice by adding tiron (an O_2^- scavenger) suggesting a role for O_2^- (Fig. 3B). The endothelium-dependent vessel relaxation to Ach (Fig. 3B) was completely blocked by adding L-NAME, an inhibitor of endothelial nitric oxide synthase (eNOS) indicating that Ach-induced vessel relaxation was depending on endothelial release of NO (Fig. 3C). However, the smooth muscle relaxation response to SNP (a NO donor) was not affected by age (Fig. 3D). The significance in reduced endothelium-dependent response to Ach in WT aging mice was further confirmed by EC50 values (Fig. 3E).

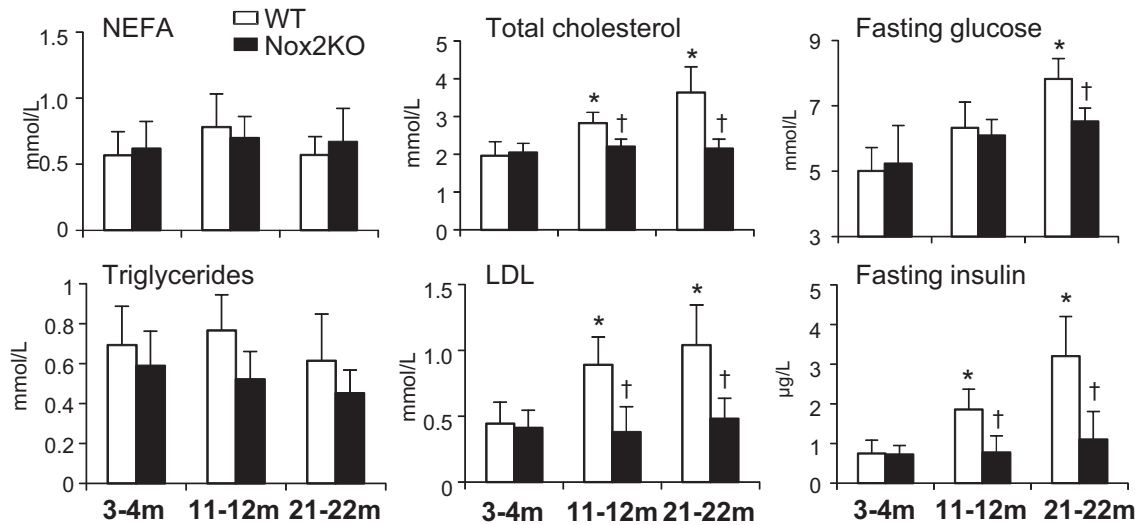
3.4. Aging-associated activation of Nox2, stress signaling pathways, VCAM-1 expression and damage of insulin receptor expression in aortas

To further define a role for Nox2 in the oxidative regulation of aging aorta function, we examined the aorta expression of Nox subunit by Western blot (Fig. 4A). Compared to young WT aortas, there were significant increases in the levels of Nox2, p22^{phox}, p40^{phox}, p47^{phox}, p67^{phox} and rac1/2 expressions, and a significant decrease in Nox4

A) Metabolic measurements



B) Lipid and glucose profile



C) Glucose tolerance test

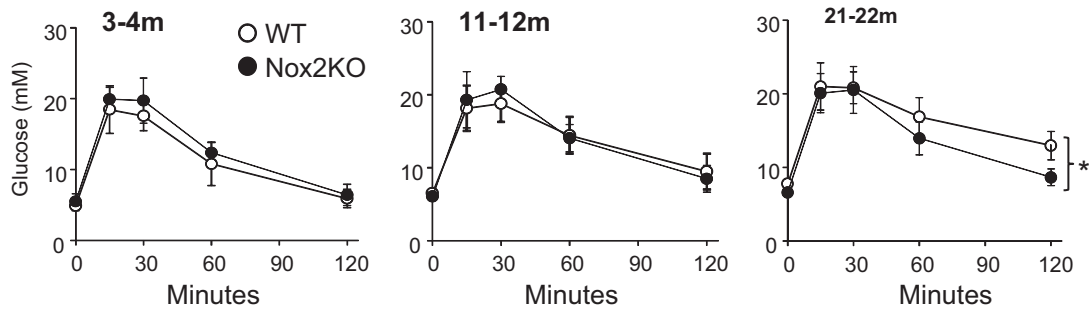


Fig. 1. Aging-associated metabolic disorders in WT and Nox2KO mice. A) and B): H/B: heart/body. *P < 0.05 for indicated values versus 3–4 m values of the same genetic group. †P < 0.05 for indicated values versus WT values of the same age group. C) Intraperitoneal glucose tolerance test. *P < 0.05 for the difference between WT and Nox2KO values (area under curve). n = 12 mice/group.

expression in aging WT aortas. However, there was no significant difference in the levels of expressions of p22^{phox}, p40^{phox}, p47^{phox}, p67^{phox} and rac1/2 between young and aging Nox2KO aortas; instead, aging Nox2KO aortas had a significant increase in Nox4 expression as compared to young Nox2KO controls (Fig. 4A). Although the levels of Nox1 expression showed a pattern of age-related increase, the differ-

ence between young and aging groups was not statistically significant for both WT and Nox2KO mice.

We then examined the difference in redox-sensitive ERK1/2, p38MAPK and JNK phosphorylation in aortic samples using phosphorylation-specific monoclonal antibodies. The levels of total protein detected in the same samples were used as loading controls (Fig. 4B).

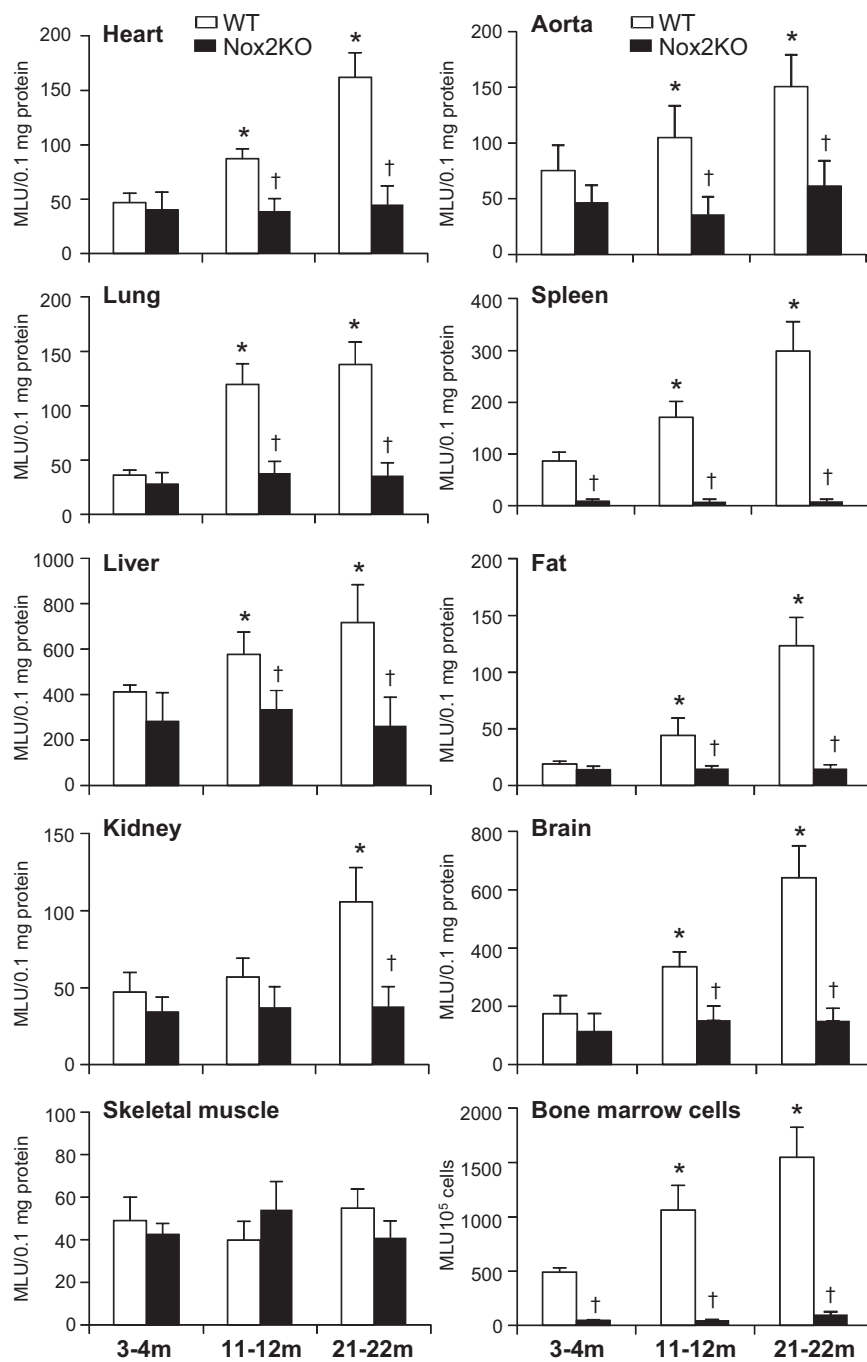


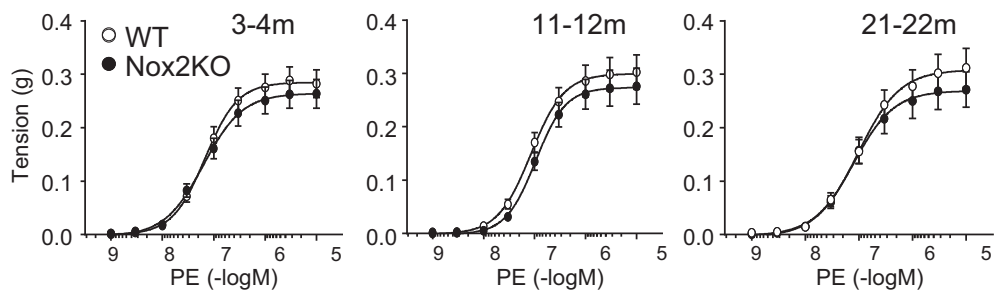
Fig. 2. Levels of O_2^- production in different organs measured by lucigenin-chemiluminescence. Tissue homogenates were used to measure NADPH-dependent O_2^- production by the heart, aorta, lung, spleen, liver, fat, kidney, brain and skeletal muscles. Living bone marrow cells were used to measuring O_2^- production (without adding NADPH) by cells. * $P < 0.05$ for indicated values versus 3–4 m values of the same genetic group. † $P < 0.05$ for indicated values versus WT values of the same age group. $n = 12$ mice/group.

Compared to young WT aortas, the levels of ERK1/2 phosphorylation were increased significantly, whereas the levels of p38MAPK phosphorylation were decreased significantly in aging WT aortas (Fig. 4B). However, there was no significant difference in ERK1/2 and p38MAPK phosphorylation between young and aging aortas of Nox2KO mice. The levels of phosphorylated JNK were very low and showed no significant change between age groups of WT and Nox2KO aortas. Putting everything together, our data strongly suggest a crucial role for age-associated Nox2 activation in the activation of redox signaling pathways in aging WT aortas.

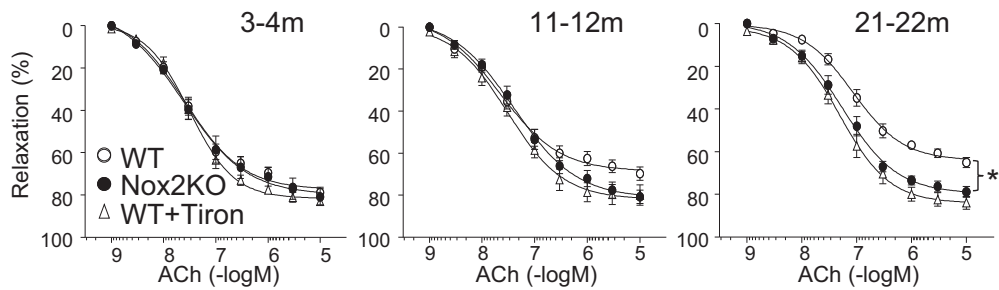
To explore any relationship between Nox2-derived oxidative stress, inflammation and vascular insulin resistance in aging aortas, we

examined the levels of expression of vascular cell adhesion molecule 1 (VCAM-1, an inflammation marker), the expression of insulin receptor and the levels of AKT phosphorylation (a key molecule involved in the insulin signaling pathway) in aortic homogenates by Western blot (Fig. 4C). There was no significant difference in the expression of these molecules at the young age between WT and Nox2KO aortas. However, there was a significant increase in the VCAM-1 expression in aging WT aortas, which was accompanied by significant decreases in insulin receptor (both IR α and IR β) expression and AKT phosphorylation in comparison to the levels in young WT aortas, (Fig. 4C). These changes were absent in Nox2KO aging aortas.

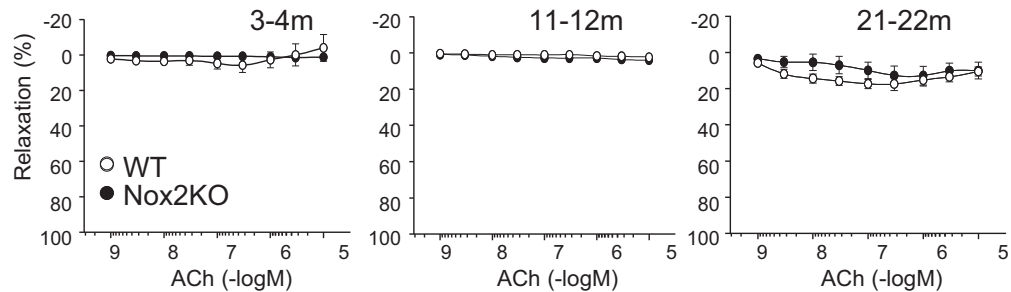
A) Constriction to PE



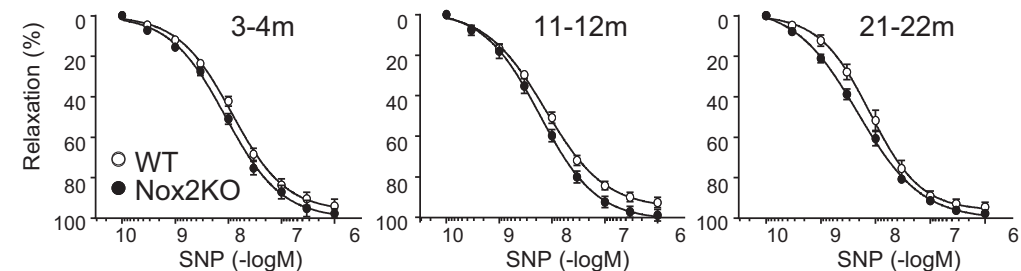
B) Relaxation to Ach



C) L-NAME effects on relaxation to Ach



D) Relaxation to SNP



E) EC50

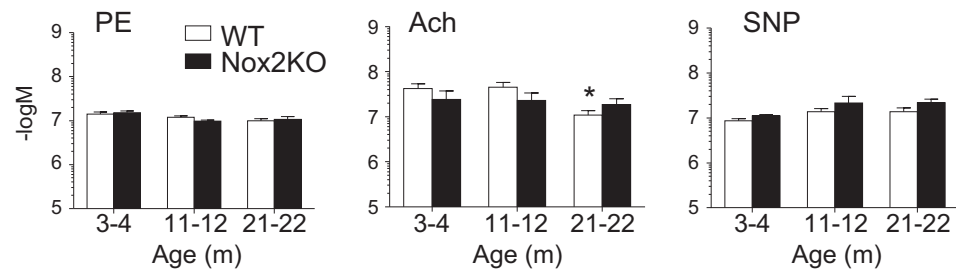


Fig. 3. Vasomotor functional assessment of aortic rings. A) PE: phenylephrine. B) Endothelium-dependent vessel relaxation response to acetylcholine (Ach). Tiron (O_2^- scavenger) was used to confirm a role of O_2^- . *P < 0.05 for significant difference between two values (area under curve). C) The effect of L-NAME on endothelium-dependent vessel relaxation to Ach. D) Endothelium-independent vessel relaxation response to SNP (a NO donor). E) EC50 values. *P < 0.05 for indicated values versus 3–4 m values in the same genetic group. n = 12 mice/group.

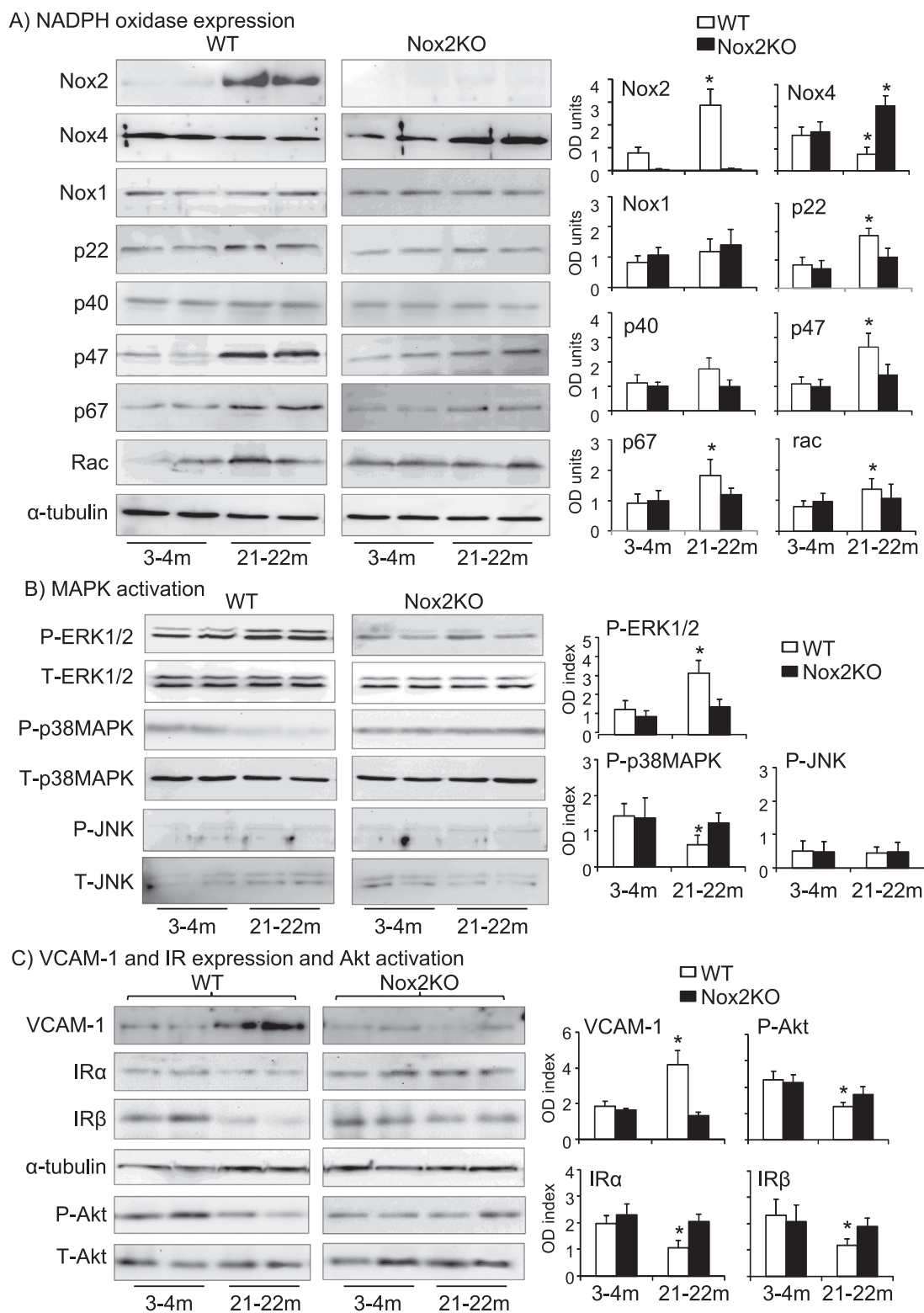


Fig. 4. Western blot detection of NADPH oxidase subunit expression, MAPK activation, VCAM-1 and insulin receptor expressions and Akt activation in aortas. A) NADPH oxidase subunit expression. Optical densities (OD) of protein bands were quantified and normalized to α -tubulin detected in the same sample. B) MAPK phosphorylation. The phospho-bands were quantified and normalized to the total levels of the same protein detected in the same samples. C) VCAM-1 and insulin receptor expression and Akt phosphorylation. Protein bands were quantified and normalized to α -tubulin detected in the same sample. * $P < 0.05$ for indicated values versus 3-4 m values in the same genetic group. $n = 9$ mice/group.

3.5. In situ detection of ROS production, Nox2 expression, inflammation and oxidative damage of insulin receptor expression in aging aortas

Increased ROS production in the aging aorta was further examined in situ by DHE fluorescence on aortic sections (Fig. 5A). Tiron was used

to confirm the detection of O_2^- . Compared to young WT vessels, there was a significant increase in DHE fluorescence throughout the aortic wall of WT aging mice, which was significantly reduced by adding tiron. In contrast, there was no significant increase in DHE fluorescence in Nox2KO aging aortas as compared to young Nox2KO aortas.

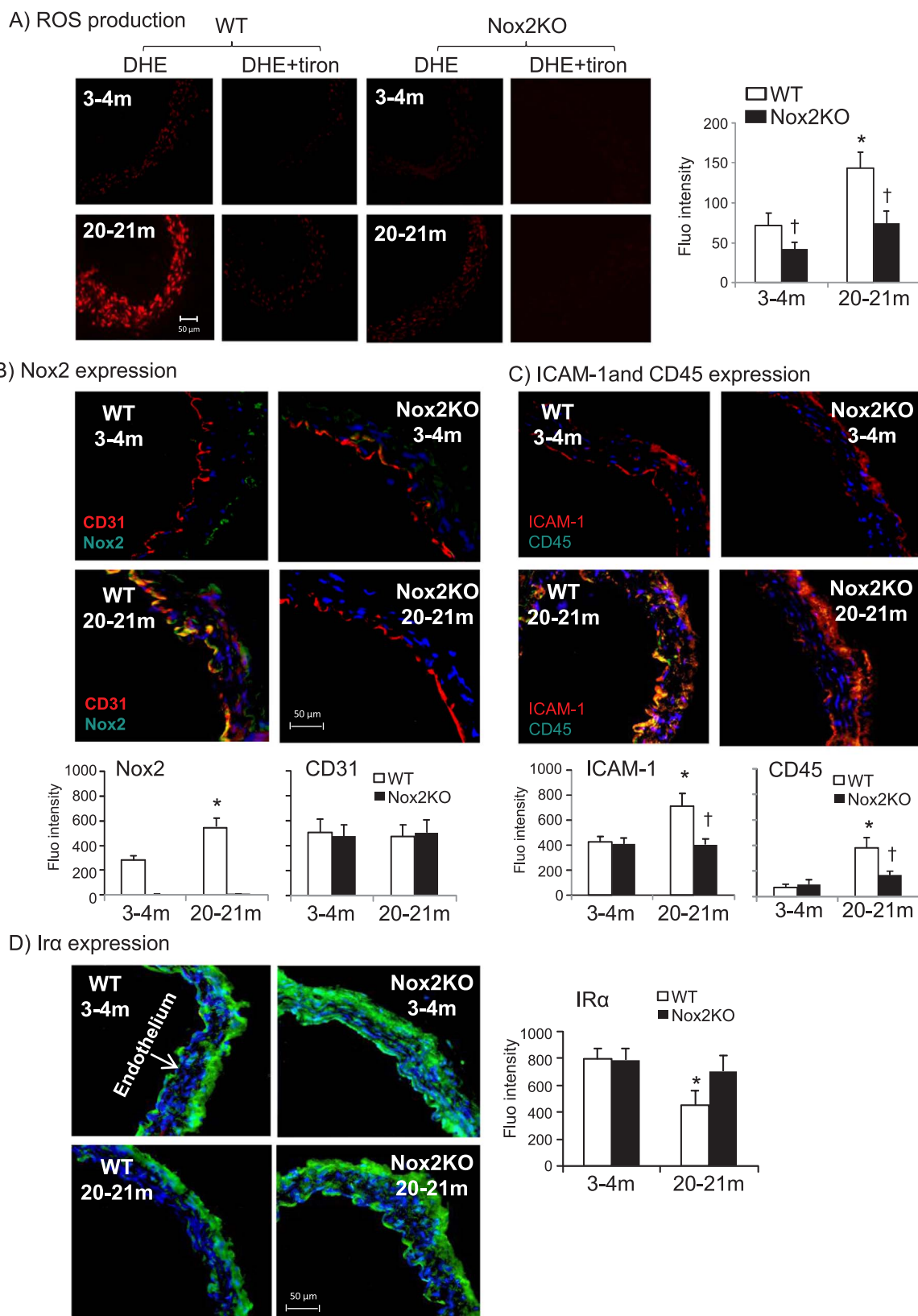


Fig. 5. Immunofluorescence detection of ROS production and the expressions of Nox2, inflammatory markers and insulin receptor in aorta walls. A) Aorta ROS production detected by in situ DHE fluorescence (red). Tiron was used to confirm the detection of O_2^- . B) Nox2 expression (green). The endothelium was labelled with CD31 (red). Endothelial expression of Nox2 was indicated by the yellow fluorescence. C) Aorta expression of inflammatory marker, ICAM-1 (red) and CD45 positive (green) inflammatory cell infiltration. D) Insulin receptor (IR α) expression. Nuclei were labelled by DAPI (blue colour) to visualize the vessel wall. *P < 0.05 for indicated values versus 3–4 m values in the same genetic group. †P < 0.05 for indicated values versus WT values from the same age group. n = 9 mice/group.

In order to confirm an increased endothelial Nox2 expression in aging aortas, we labelled the endothelium with CD31 (an endothelial cell marker, red fluorescence) and detected Nox2 expression (green fluorescence) in aortic sections. Nuclei were labelled with DAPI (blue fluorescence) to visualize the cells (Fig. 5B). Nox2 was weakly detectable in WT young aortas and was mainly present in the adventitia. Compared to WT young aortas, there was a significant increase in endothelial Nox2 expression in aging WT aortas as indicated by the yellow fluorescence (Fig. 5B).

Endothelial inflammation was further examined by the expression of intercellular adhesion molecule-1 (ICAM-1, red) and infiltrating leucocytes (labelled with CD45, green) (Fig. 5C). At young age, the level of ICAM-1 expression was low and mainly detected in the endothelium and adventitia without significant difference between WT and Nox2KO mice; CD45-positive cells were almost undetectable in the aortic wall of both WT and Nox2KO young mice. However, at old age, there was a remarkable increase in the levels of ICAM-1 expression in the endothelium of WT aortas, and this was accompanied by CD45-positive leucocyte infiltration throughout the vessel wall predominately around the endothelium as indicated by the yellow fluorescence (Fig. 5C). However, these inflammatory changes were significantly reduced in Nox2KO aging aortas.

We then examined the aorta insulin receptor expression (Fig. 5D). Insulin receptor α was detected throughout the aortic wall without significant difference at young age between WT and Nox2KO mice. Compared to young WT aortas, the expression of insulin receptor α was reduced significantly in WT aging aortas mainly in the endothelium and the media. However, insulin receptor expression was well preserved in aging Nox2KO aortas.

3.6. Metabolic disorder-induced Nox2 activation and oxidative damage of endothelial function in high fat diet (HFD)-induced obesity and insulin resistance treated with or without apocynin

High-fat diet-induced mouse model of obesity and insulin resistance has been shown to display an accelerated aging phenotype and increased levels of oxidative stress/damage in organ function [21]. Therefore, it would be a good model for us to examine the effects of metabolic disorders on Nox2 activation and endothelial dysfunction. Compared to control chow diet-fed mice, WT mice under HFD increased significantly the body weight and blood pressure together with high levels of fasting serum glucose and insulin (Fig. 6A). However, these changes were significantly reduced after apocynin treatment.

We then examined the Nox2 expression in aortas by immunofluorescence. Compared to control vessels, HFD up-regulated significantly the Nox2 expression (green colour) in the aorta wall mainly in the endothelium (labelled by CD31 in red) and the adventitia (Fig. 6B). Apocynin treatment had no statistically significant effect on aorta Nox2 expression (Fig. 6B, right panel). Aortas of HFD mice had significantly higher levels of NADPH-dependent O_2^- production as examined by both lucigenin-chemiluminescence and SOD-inhibitable cytochrome c reduction assay, and these were significantly inhibited by apocynin-treatment (Fig. 6C). The endothelium-dependent vessel relaxation to acetylcholine was attenuated in HFD WT aortas, and this was well preserved in HFD mice treated with apocynin (Fig. 6D). The impairment of endothelium-dependent vessel relaxation to acetylcholine in HFD WT aorta was inhibited by MnTMPyP (a cell permeable SOD mimic), which further confirmed the role of ROS in mediating HFD-induced endothelial dysfunction (Fig. 6D, right panel).

3.7. High glucose and insulin-induced endothelial Nox2 activation and oxidative signaling in endothelial cell senescence and apoptosis

Hyperglycaemia and hyperinsulinaemia-induced Nox2 activation and stress signaling in endothelial aging was further examined using CMECs isolated from middle-aged (11–12 m) WT and Nox2KO mice.

Cells were challenged with high glucose (25 mmol/L) plus insulin (1.2 nmol/L) for 24 h and examined for NADPH-dependent O_2^- production (Fig. 7A). Compared to vehicle-stimulated control cells, high glucose/insulin significantly increased the levels of O_2^- production in WT cells (Fig. 7A, left panel), and this was inhibited significantly by tiron and DPI (a flavoprotein inhibitor), but not by L-NAME (NOS inhibitor), rotenone (mitochondria complex 1 enzyme inhibitor) nor oxypurinol (xanthine oxidase inhibitor) (Fig. 7A, right panel). Increased ROS production by WT CMECs was accompanied by significant increases in the levels of Nox2 expression, ERK1/2 phosphorylation and p53 (cell apoptosis-related gene product) expression (Fig. 7B). In contrast, Nox2KO CMECs failed ROS response to high glucose/insulin challenge (Fig. 7A, middle panel), and the ERK1/2 and p53 activation were inhibited or absent in Nox2KO cells (Fig. 7B). The role of Nox2-derived ROS in mediating endothelial senescence and apoptosis was examined by SA β G activity and TUNEL assay, respectively (Fig. 7C). In comparison to WT control cells, high glucose/insulin challenge significantly increased the levels of intracellular ROS production detected by DCF fluorescence (green, left panels), and this was accompanied by significant increases in Nox2 expression (green, middle left panels), cell senescence (blue, middle right panels) and cell apoptosis (yellow, right panels). However, these changes were significantly inhibited in Nox2KO cells.

4. Discussion

Aging is recognized as a normal biological process and is often associated with progressive oxidative stress in multiple organs [2,3]. Although accumulating evidence has suggested that Nox2-derived ROS are involved in the oxidative damage of vascular function, the mechanisms (or factors) of Nox2 activation in normal aging remain unclear. This report using WT and Nox2KO mice of three distinct age groups (3–4 m, 11–12 m and 21–22 m) combined with a range of cellular and molecular approaches, revealed for the first time a crucial role for metabolic disorders (in particular hyperglycaemia and hyperinsulinaemia secondary to insulin resistance) in systemic Nox2 activation, vascular inflammation and endothelial dysfunction in aging.

One of the common pathophysiological manifestations in human aging is a declining regulation of glucose metabolism [3,22]. In accordance with previous reports, we found that WT mice developed hyperglycaemia and hyperinsulinaemia starting in middle age and worsening at old age, when the levels of fasting serum glucose and insulin were nearly two-fold and four-fold of the levels of WT young mice, respectively. The novelty of the current study is that we showed a global Nox2 activation (not restricted in the endothelium) in response to aging-associated hyperglycaemia and hyperinsulinaemia as demonstrated by an age-related increase in the levels of Nox2-derived ROS production in several vital organs of WT mice including the heart, aorta, lung, spleen, kidney, brain, and bone marrow. We also demonstrated a positive feedback loop between progressive Nox2 activation in a high glucose/insulin environment and Nox2-derived oxidative stress causing further damage to the global metabolism in aging. Knockout of Nox2 or inhibiting Nox2 not only reduced the levels of aging-associated ROS production in these organs but also prevented metabolic syndrome and preserved endothelial function in old age.

Mouse aorta is a well-established and mostly used organ for studying metabolic or aging-related large vessel dysfunction [23]. An important discovery in the current study is that reduced IR expression and IR signaling (Akt phosphorylation) in aging aortas together with inflammation and oxidative damage of endothelial function. Using three complementary techniques (lucigenin-chemiluminescence, in situ DHE fluorescence and SOD-inhibitable cytochrome c reduction assay), we demonstrated that aging aortas produced ~2 folds more ROS than young controls and this was accompanied by profound endothelial dysfunction and high blood pressure. The impaired endothelial dependent vessel relaxation was related to oxidative stress because addition of superoxide

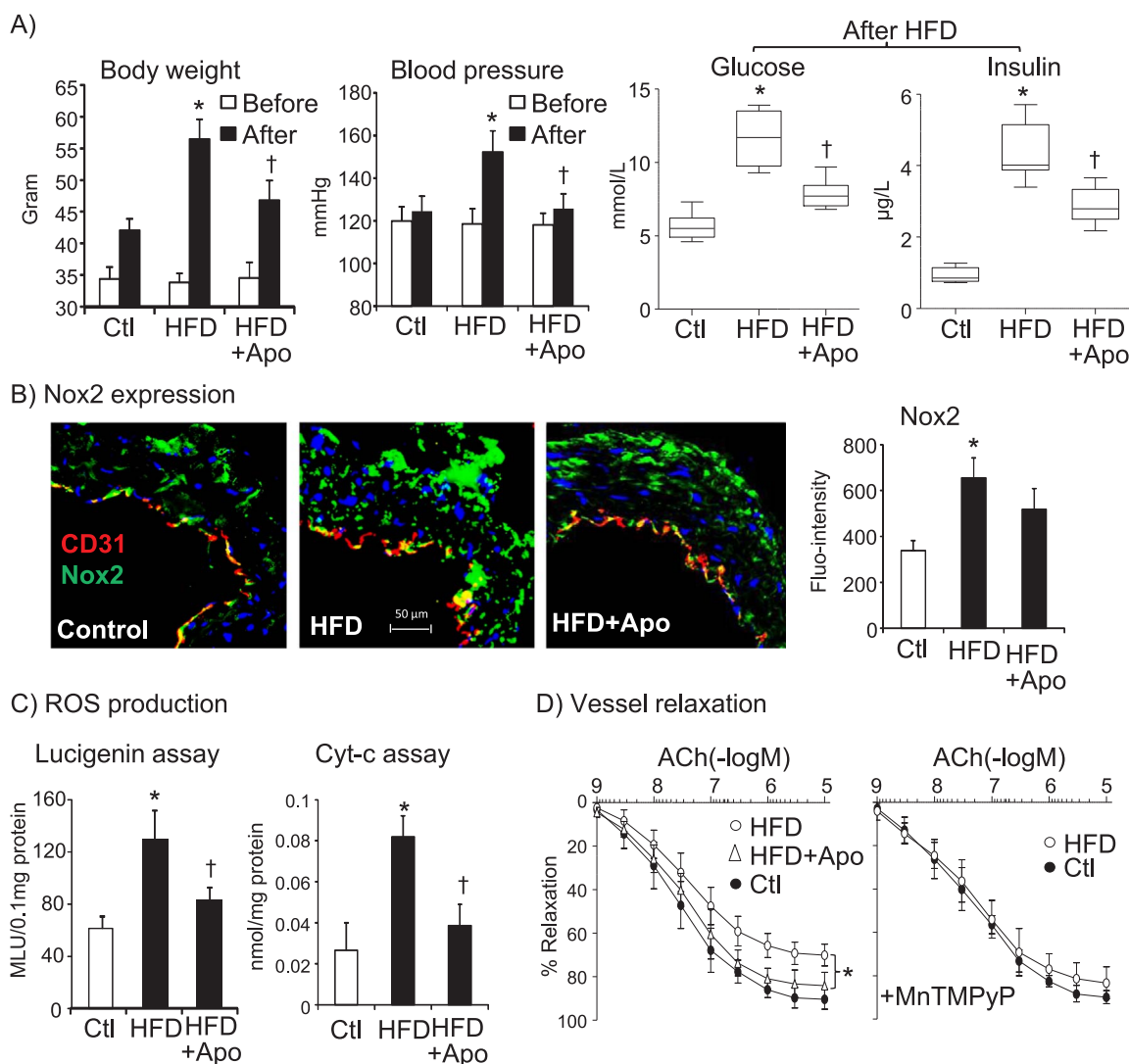


Fig. 6. Metabolic disorder-induced Nox2 activation and endothelial dysfunction in high fat-diet (HFD)-induced obesity and insulin-resistance treated with or without apocynin. A) Metabolic measurements. B) Immunofluorescence detection of Nox2 (green) in aortic wall sections. The endothelium was labelled with CD31 (red). Endothelial expression of Nox2 was indicated by the yellow fluorescence. C) Aorta ROS production detected by lucigenin-chemiluminescence and SOD-inhibitable Cytochrome c reduction assay. *P < 0.05 for HFD values versus control (Ctl) values after dietary intervention. †P < 0.05 for indicated values versus HFD values after dietary intervention. D) Endothelium-dependent vessel relaxation response to acetylcholine (Ach). *P < 0.05 for significant difference between two values (area under curve). n = 9 mice per group.

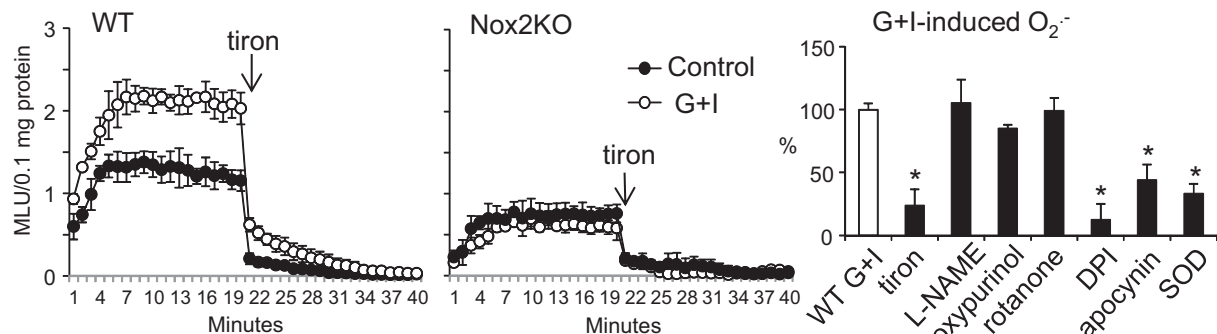
scavenger (tiron or MnTlMPyP) in the organ bath restored the endothelial function. Furthermore, knockout of Nox2 completely abolished aorta ROS production and restored IR expression and signaling in old age. The crucial role of metabolic disorder-induced Nox2 activation and oxidative damage of endothelial function was further demonstrated using an accelerated aging model of HFD-induced obesity and insulin resistance of mice at 12 m of age, which is equivalent to a human of ~50 years old when most metabolic and vascular diseases occur [1,21,23]. Once again we showed that inhibition of Nox2 activity using apocynin significantly reduced HFD-induced high blood pressure and aorta oxidative stress and preserved endothelial function.

High glucose and insulin are potent activators of the endothelial Nox2 enzyme [3,4]. The current study extends our understanding of insulin resistance in vascular aging by showing that high glucose/insulin via Nox2 stress signaling pathways promotes premature endothelial cell aging. In response to high glucose and insulin challenge, WT endothelial cells increased ROS production, which resulted in ERK1/2 activation, p53 expression and endothelial cell senescence and apoptosis. Knockout of Nox2 not only abolished high glucose/insulin-induced ROS production but also protected endothelial cells from premature senescence and apoptosis. Although the relevance of in

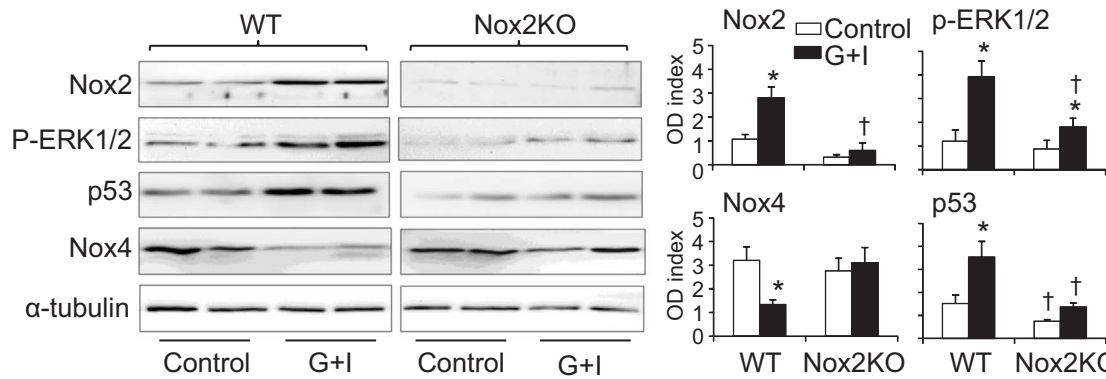
vitro senescence to organismal aging remains unclear, our in vitro data are in support of our in vivo observation that Nox2 plays a crucial role in glucose metabolic disorder-associated oxidative damage of endothelial cells and vascular aging.

The catalytic subunit of NADPH oxidase has 7 isoforms viz. Nox1-5, and Duox1-2 [24]. Among these Nox isoforms, Nox2 and Nox4 are largely expressed in the endothelium [6,25]. Nox2 has been found to be involved in vascular inflammation and atherosclerotic lesion formation [26], whereas Nox4 has been reported to play a protective role in vascular function [27]. The current study extended our understanding of NADPH oxidase by showing an aging-associated increase in Nox2 expression and a decrease in Nox4 expression in WT aging aortas. The mirror image of Nox2 and Nox4 expressions in aging aortas were accompanied by a significant increase in ERK1/2 activation and reduction in p38MAPK activation. Although the redox-signaling pathways underlying vascular aging remain unclear, it is possible that Nox2 signaling through ERK1/2 is involved in aging-associated deterioration of endothelial function. However, in the absence of Nox2, we found a significant increase of Nox4 expression in aging Nox2KO aorta, which might be a compensatory response. Compensatory increase in Nox4 in the deficiency of Nox2 had been reported previously in endothelial cells

A) ROS production



B) Nox2 and p53 expression



C) Endothelial cell senescence and apoptosis

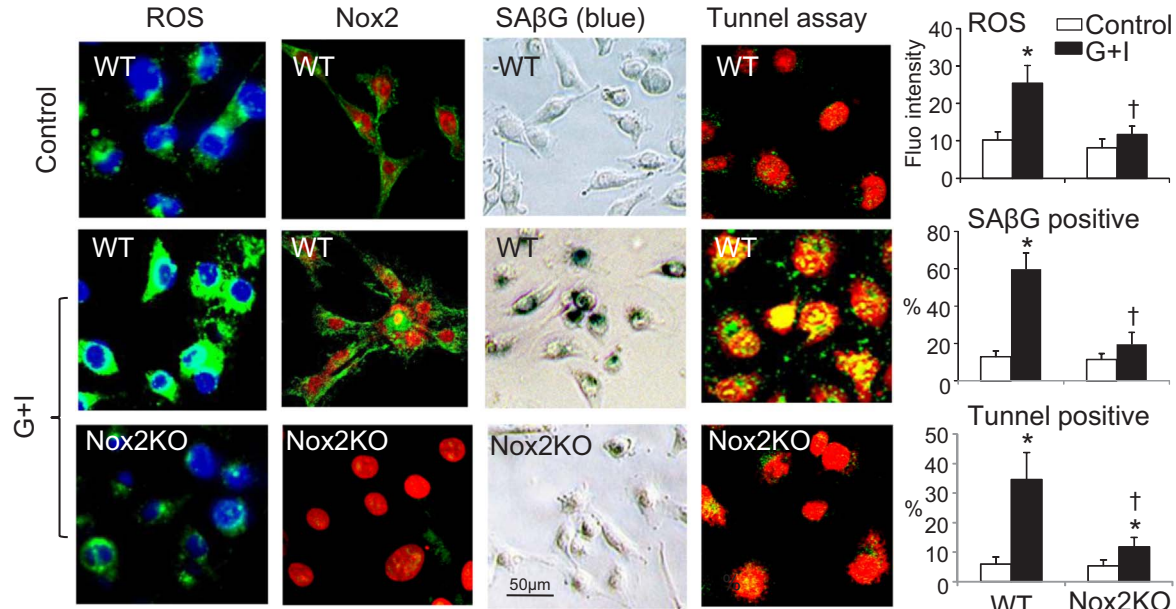


Fig. 7. High glucose and insulin-induced Nox2 activation and stress signaling in cell senescence and apoptosis in primary coronary microvascular endothelial cells. A) Luciferase chemiluminescence. Tiron was used to confirm the detection of O_2^- . Right panel: The effects of different enzyme inhibitors on high glucose and insulin (G+I)-induced O_2^- production by WT CMEC. *P < 0.05 for indicated values versus WT G+I value. B) Western blot. C) Left panels: *In situ* DCF (green) fluorescence detection of intracellular ROS production. Nuclei were labelled with DAPI (blue). Left middle panels: Nox2 expression (FITC, green). Nuclei were labelled with propidium iodide (red). Right middle panels: Cell senescence was detected by SA β G activity (blue) and visualised under light microscopy. Right panels: cell apoptosis detected by TUNEL assay. Apoptotic cells were labelled by the yellow fluorescence. SA β G and TUNEL positive cells were expressed as percentage of total cells. *P < 0.05 for indicated values versus control values in the same genetic groups. †P < 0.05 for indicated values versus WT G+I values. n = 3 separate CMEC isolation/group. Six mice were used for each CMEC isolation.

[28,29]. Although skeletal muscle atrophy and reduced strength are common inevitable features of aging [30], Nox2 is not involved because knockout of Nox2 had no significant effect on the amount of O_2^- production by skeletal muscles regardless of age.

In summary, we have reported in the current study a crucial role for

Nox2-containing NADPH oxidase activation in response to aging-associated metabolic disorders in mediating systemic oxidative stress and oxidative damage of endothelial function and insulin receptor function. Inhibition or knockout of Nox2 preserves endothelial function and delays vascular aging.

Founding

This work was supported by the research grants from the AgeUK (grant number: RIA 359) and the British Heart Foundation (grant number: PG/14/85/3116) awarded to JML.

Conflict of interest

No conflict of interest to declare.

References

- [1] D.K. Houston, B.J. Nicklas, C.A. Zizza, Weighty concerns: the growing prevalence of obesity among older adults, *J. Am. Diet. Assoc.* 109 (2009) 1886–1895.
- [2] K.H. Krause, Aging: a revisited theory based on free radicals generated by NOX family NADPH oxidase, *Exp. Gerontol.* 42 (2007) 256–262.
- [3] T. Finkel, N.J. Holbrook, Oxidants, oxidative stress and the biology of aging, *Nature* 408 (2000) 239–247.
- [4] P. Sukumar, H. Viswambharan, H. Imrie, R.M. Cubbon, N. Yuldasheva, M. Gage, S. Galloway, A. Skromna, P. Kandavelu, C.X. Santos, V.K. Santos, J. Smith, D.J. Beech, S.B. Wheatcroft, K.M. Channon, A.M. Shah, M.T. Kearney, Nox2 NADPH oxidase has a critical role in insulin resistance-related endothelial cell dysfunction, *Diabetes* 62 (2013) 2130–2134.
- [5] E.R. Duncan, S.J. Walker, V.A. Ezzat, S.B. Wheatcroft, J.-M. Li, A.M. Shah, M.T. Kearney, Accelerated endothelial dysfunction in mild prediabetic insulin resistance: the early role of reactive oxygen species, *Am. J. Physiol. Endocrinol. Metab.* 293 (2007) E1311–E1319.
- [6] J.-M. Li, A.M. Shah, Endothelial cell superoxide generation: regulation and relevance for cardiovascular pathophysiology, *Am. J. Physiol. Regul. Integr. Comp. Physiol.* 287 (2004) R1014–R1030.
- [7] L.M. Fan, G. Douglas, J.K. Bendall, E. McNeil, M.J. Crabtree, A.B. Hale, A. Mai, J.-M. Li, M.A. McAteer, J.E. Schneider, R.P. Choudhury, K.M. Channon, Endothelial cell-specific ROS production increases susceptibility to aortic dissection, *Circulation* 129 (2014) 2661–2672.
- [8] J. Du, L.M. Fan, A. Mai, J.-M. Li, Crucial roles of Nox2-derived oxidative stress in deteriorating the function of insulin receptor and endothelium in dietary obesity of middle-aged mice, *Br. J. Pharmacol.* 170 (2013) 1064–1077.
- [9] J.D. Lambeth, G. Cheng, R.S. Arnold, W.A. Edens, Novel homologs of gp91phox, *Trends Biochem. Sci.* 25 (2000) 459–461.
- [10] B. Lassègue, A.S. Martin, K.K. Gründling, Biochemistry, physiology, and pathophysiology of NADPH oxidase in the cardiovascular system, *Circ. Res.* 110 (2012) 1364–1390.
- [11] H. Sumimoto, K. Miyano, R. Takeya, Molecular composition and regulation of the Nox family NAD(P)H oxidases, *Biochem. Biophys. Res. Commun.* 338 (2005) 677–686.
- [12] B.C. Capell, F.S. Colins, E.G. Nabel, Mechanisms of cardiovascular disease in accelerated aging syndromes, *Circ. Res.* 101 (2007) 13–26.
- [13] J.D. Pollock, D.A. Williams, M.A. Gifford, L.L. Li, X. Du, J. Fisherman, S.H. Orkin, C.M. Doerschuk, M.C. Dinauer, Mouse model of X-linked chronic granulomatous disease, an inherited defect in phagocyte superoxide production, *Nat. Genet.* 9 (1995) 202–209.
- [14] N. Abudu, S.S. Levinson, Calculated low-density lipoprotein cholesterol remains a viable and important test for screening and targeting therapy, *Clin. Chem. Lab. Med.* 45 (2007) 1319–1325.
- [15] J.-M. Li, A.M. Mullen, A.M. Shah, Phenotypic properties and characteristics of superoxide production by mouse coronary microvascular endothelial cells, *J. Mol. Cell. Cardiol.* 33 (2001) 1119–1131.
- [16] C.L. Kao, L.K. Chen, Y.L. Chang, M.C. Yung, C.C. Hsu, Y.C. Chen, W.L. Lo, S.J. Chen, H.H. Ku, S.J. Hwang, Resveratrol protects human endothelium from H(2)O(2)-induced oxidative stress and senescence via SirT1 activation, *J. Atheroscler. Thromb.* 17 (2010) 970–979.
- [17] L. Fan, D. Sawbridge, V. George, L. Teng, A. Bailey, I. Kitchen, J.-M. Li, Chronic cocaine-induced cardiac oxidative stress and mitogen-activated protein kinase activation: the role of Nox2 oxidase, *J. Pharmacol. Exp. Ther.* 328 (2009) 99–106.
- [18] L.M. Fan, J.-M. Li, Evaluation of methods of detecting cell reactive oxygen species production for drug screening and cell cycle studies, *J. Pharmacol. Toxicol. Methods* 70 (2014) 40–47.
- [19] S. Molshanski-Mor, A. Mizrahi, Y. Ugolev, I. Dahan, Y. Berdichevsky, E. Pick, Cell-free assays: the reductionist approach to the study of NADPH oxidase assembly, or "all you wanted to know about cell-free assays but did not dare to ask", *Methods Mol. Biol.* 412 (2007) 385–428.
- [20] S. Thakur, J. Du, S. Hourani, C. Ledent, J.-M. Li, Inactivation of adenosine A2_A receptor attenuates basal and angiotensin II-induced ROS production by Nox2 in endothelial cells, *J. Biol. Chem.* 285 (2010) 40104–40113.
- [21] Y. Zhang, K.E. Fischer, V. Soto, Y. Liu, D. Sosnowska, A. Richardson, A.B. Salmon, Obesity-induced oxidative stress, accelerated functional decline with age and increased mortality in mice, *Arch. Biochem. Biophys.* 576 (2015) 39–48.
- [22] F.L. Muller, M.S. Lustgarten, Y. Jang, A. Richardson, H. Van Remmen, Trends in oxidative aging theories, *Free Rad. Biol. Med.* 43 (2007) 477–503.
- [23] F. Kim, M. Pham, E. Maloney, N.O. Rizzo, G.J. Morton, B.E. Wisse, E.A. Kirk, A. Chait, M.W. Schwartz, Vascular inflammation, insulin resistance, and reduced nitric oxide production precede the onset of peripheral insulin resistance, *Atheroscler. Thromb. Vasc. Biol.* 28 (2008) 1982–1988.
- [24] S.H. Bengtsson, L.M. Gulluyan, G.J. Dusting, G.R. Drummond, Novel isoforms of NADPH oxidase in vascular physiology and pathophysiology, *Clin. Exp. Pharmacol. Physiol.* 30 (2003) 849–854.
- [25] R.P. Brandes, J. Kreuzer, Vascular NADPH oxidases: molecular mechanisms of activation, *Cardiovasc. Res.* 65 (2005) 16–27.
- [26] A. Konior, A. Schramm, M. Czesnikiewicz-Guzik, T.J. Guzik, NADPH oxidases in vascular pathology, *Antioxid. Redox Signal.* 20 (2014) 2794–2814.
- [27] K. Schröder, M. Zhang, S. Benkhoff, A. Mieth, R. Pliquet, J. Kosowski, C. Kruse, P. Luedike, U.R. Michaelis, N. Weissmann, S. Dommeler, A.M. Shah, R.P. Brandes, Nox4 is a protective reactive oxygen species generating vascular NADPH oxidase, *Circ. Res.* 110 (2012) 1217–1225.
- [28] S. Pendyala, I.A. Gorshkova, P.V. Usatyuk, D. He, A. Pennathur, J.D. Lambeth, V.J. Thannickal, V. Natarajan, Role of Nox4 and Nox2 in hyperoxia-induced reactive oxygen species generation and migration of human lung endothelial cells, *Antioxid. Redox Signal.* 11 (2009) 747–764.
- [29] J.-M. Li, L.M. Fan, V.T. George, G. Brooks, Nox2 regulates endothelial cell cycle arrest and apoptosis via p21^{ip1} and p53, *Free Radic. Biol. Med.* 43 (2007) 976–986.
- [30] M.J. Jackson, Interactions between reactive oxygen species generated by contractile activity and aging in skeletal muscle? *Antioxid. Redox Signal.* 19 (2013) 804–812.